ISSN 1392 - 1207. MECHANIKA. 2012 Volume 18(6): 624-631

On the strength problem in chain elements overloaded during maintenance of bio-fuel conveyor

A. Žiliukas*, S. Diliūnas, A. Jutas***, S.V. Augutis****, R. Ramanauskas*******

**Kaunas University of Technology, Kęstučio St.27, 44312 Kaunas, Lithuania, E-mail: antanas.ziliukas@ktu.lt*
***Kaunas University of Technology, Kęstučio St.27, 44312 Kaunas, Lithuania, E-mail: saulius.diliunas@ktu.lt*
****Kaunas University of Technology, Kęstučio St.27, 44312 Kaunas, Lithuania, E-mail: audrius.jutas@ktu.lt*
*****Kaunas University of Technology, Studentų St. 50, 51368 Kaunas, Lithuania, E-mail: stasys.augutis@ktu.lt*
******Kaunas University of Technology, Studentų St. 50, 51368 Kaunas, Lithuania, E-mail: ramunas.ramanauskas@ktu.lt*

crossref http://dx.doi.org/10.5755/j01.mech.18.6.3171

Nomenclature

φ – angle between chain axis and conveyor frame or angle of chain distortion, degrees; F_H and F_I – chain tensile forces caused by chain own weight on horizontal and inclined parts, respectively, N; F_{HM} and F_{IM} – chain tensile forces caused by chain own weight and weight of conveyed material on horizontal and inclined parts, respectively, N; k_i – experimental coefficient depending on inertia of moving chain [3]; f_r – coefficient of rolling resistance; c – experimental coefficient depending on material and surface roughness of the areas of contact; f_{sd} and f_{sw} – coefficient of sliding friction between chain and conveyor material according to dry and wet operational conditions, respectively; f_{sM} – coefficient of sliding friction between material to be conveyed and steel; N – number of chain strands; $p(y)$ – investigated chain distance, mm; α – angle of inclination of conveyor, degrees; q – one meter chain mass, kg/m; m_h and m_b – masses of scrapper holder and bolt join, respectively, kg; m_p and m_a – masses of scrapper plate and angle, respectively, kg; n_H ir n_I – number of scrappers on horizontal and inclined chain, respectively; g – acceleration of gravity, m/s; B, P, S – one section width, length and depth, respectively, mm; ρ – bulk weight of material to be conveyed kg/m^3; k_f – ratio evaluating filling of conveyor by biofuel; ψ – filling ratio of material to be conveyed; ϕ – ratio evaluating contact degree of sliding friction, if chain contacts with conveyor frame; L_c – chain length, that contacts with conveyor frame, m; L_H, L_I – horizontal and inclined conveying lengths, respectivelly, m; s – chamfer width of sprocket tooth, mm; $F_s(\varphi)$– transversal force, N; $M(F_s)$ – bending moment, Nm; r_{ex} and r_{in} – external and internal radii of axle, respectively, mm; ξ – coefficient of contamination by wood chips between inner surface of roller and external surface of axle; σ_{avg} – averraging normal stress of bearing, Pa; σ_b – bending normal stress, MPa; σ_{eq} – equivalent normal stress, MPa; σ_υ – von-Misses normal stress, MPa.

1. Introduction

Lithuanian power economies increasingly use different kind of wood chips as the fuel for heat energy. Small deviations in maintenance conditions of chains influence on other cases of deformations that usually are not presented in the chain maintenance guide [1]. According to Environmental Performance Index (EPI) Lithuania was seventeenth during years 2011 [2]. It should be mentioned that the police categories such like effects of power economies on human health or ecosystem effects were also included in that analysis [3].

Usually, mentioned plants operate chain-scraper conveyors [4]. Conveyor chains equipped with rollers are designed by DIN 8167/8168. From the chain strength point of view, there are presented investigation and possible maintenance problems that change normal operational conditions, also shorten operational time of conveyor. The question was: "What reasons do influence on chain failure?" [5]. Therefore, the main aim of this investigation was to find out the reasons of possible accident. This work was carried out in three stages: 1) visual inspection of working conditions and analysis of working drawings; 2) voltage/current measurements of motor, temperature on chain joins; 3) evaluation of incidental reasons on the accidental failure. In this investigation, measurements were performed as verification for presented methodology.

2. Computation method

For the presented strength analysis the geometric and analytical models were created. The chain then is loaded by the following loads: 1) tensile load that comes from the own weight of chain and conveyed material; 2) transversal force coming from the distortion of chain because of possible incidental operational conditions; 3) bending moment coming from the action of transversal force. These loads were superposed on the evaluating chain members having the aim to simulate real operational conditions. Fig. 1 represents principal kinematic and computational scheme indicating some cases of incidental operation that may be separated to different levels of problem formulation Eq. (2).

In the case of damaged scrapper with parameter y_{max}, initial conveyor width B becomes shorter and then equals B_1

$$B_1 = b_1 + b_2 = c_1 cos\left(arcsin\frac{y_{max}}{c_1}\right) + c_2 cos\left(arcsin\frac{y_{max}}{c_2}\right) \quad (1)$$

and then chain parameter is $\Delta B = B_1 - B$.

Trying to describe possible situations of scrapper maintenance the following boundary conditions were used

$$\begin{cases} \text{I. if } c_1 = b_1,\ c_2 = b_2,\ y_{max} = 0 \text{ and } \Delta B = 0, \\ \text{then } \varphi = 0; \\ \text{II. if } c_1 > c_2,\ b_1 > b_2,\ y_{max} \neq 0 \text{ and } \Delta B \neq 0, \\ \text{then } |\varphi| > 0; \\ \text{III. if } c_1 < c_2,\ b_1 < b_2,\ y_{max} \neq 0 \text{ and } \Delta B \neq 0, \\ \text{then } |\varphi| > 0; \\ \text{IV. if } B_1 = B_0,\ y_{max} = 0 \text{ and } \Delta B = 0, \\ \text{then } |\varphi| > 0 \end{cases} \quad (2)$$

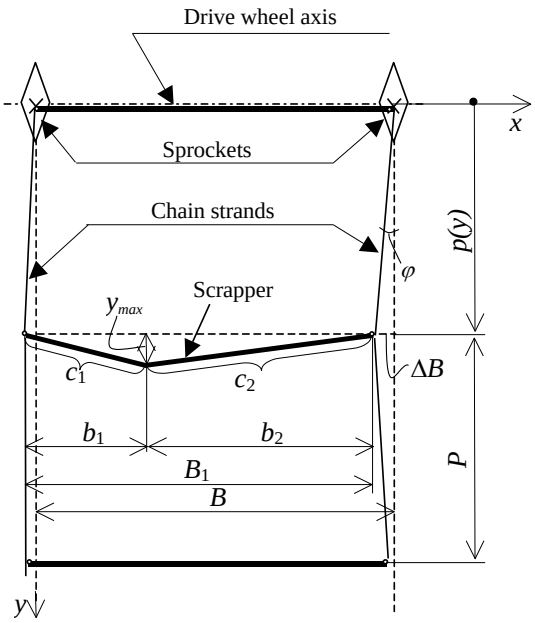

Fig. 1 Principal kinematic scheme and used geometrical parameters

As it could be seen from the Eq. (2), there are four incidental cases explaining the change in geometric parameters:

Case I: There is normal maintenance situation, the chain has no distortion $\varphi = 0$ because scrapper isn't damaged yet – $y_{max} = 0$;

Case II: A possible situation of incidental operation, conveyor scrapper is deflected at the right, $|\varphi| > 0$;

Case III: A possible situation of incidental operation, conveyor scrapper is deflected at the left, $|\varphi| > 0$;

Case IV: This is also distortion of chain with angle $|\varphi| > 0$ without scrapper deflection ($y_{max} = 0$). This situation is possible in the case of lengthening of one chain strand because of asymmetric distribution of conveyed material.

Regarding the cases mentioned above the chain may be distorted also one may have a contact with the right or left borders of conveyor.

For single chain strand chain distortion angle φ evaluates scrapper length change $\Delta B/2$, if scrapper goes to the sprocket teeth with chain pitch $p(y)$

$$\varphi = arctg \frac{\Delta B}{2p(y)} \quad (3)$$

Chain distortion angle φ increases if the narrower chain segment slides on the chamfer width of sprocket tooth s (Fig. 2)

$$\varphi_s = arctg \frac{\Delta B/2 + s}{p(y)} \quad (4)$$

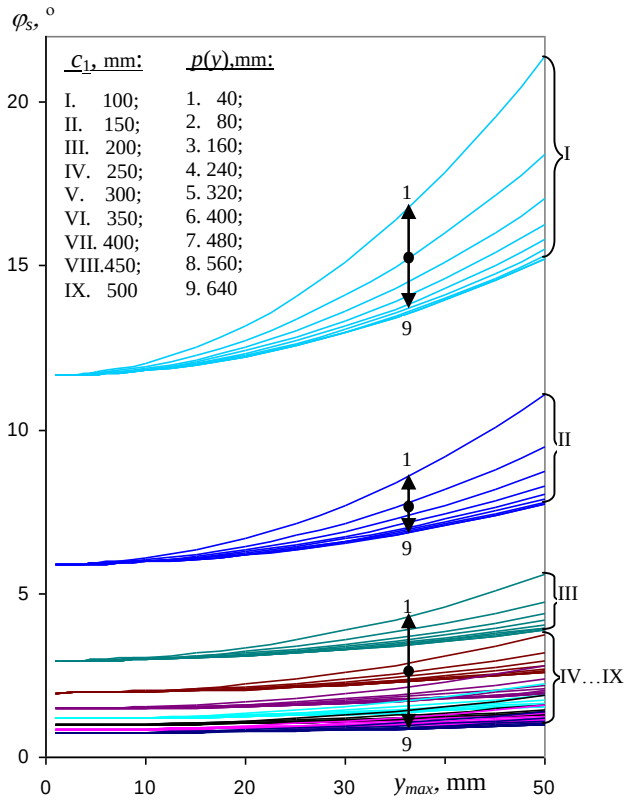

Fig. 2 Chain distortion angle φ_s versus scrapper deflection depth y_{max} influenced by c_1 and $p(y)$

From Eq. (1) obtained some decrease in conveyor section width B_1 gives us difference $\Delta B = B_1 - B$ where one half of it equal $\Delta B/2$. At investigated chain distance $p(y)$ position 1 (scrapper is close to the sprocket teeth), maximal value φ is possible as it may be seen in Fig. 2. Such value depends also on deflection position c_1 accordingly chosen Roman numbers I…IX. The structural difference in chain segments was taken into account with the use of chamfer width of sprocket tooth chamfer s. In this case chain has the narrower and wider segment. The narrower segment of chain slides on sprocket tooth chamfer s and chain distortion parameter becomes $\Delta B/2 + s$ while the wider segment of chain slides freely on sprocket tooth and distortion parameter becomes $\Delta B/2$.

As we can see from Fig. 3, the contact between the narrower segment of chain and sprocket tooth chamfer s increases distortion value by $\Delta B/2 + s$. In the next investigation, deflection position c_1 was chosen to be I, that is, $c_1 = 100$ mm. Then variable parameter was the changing chain distance $p(y)$.

2.1. Tensile force of the chain

Weight force of chain depends on the sum of masses of individual chain components and equals

$$F_c = \sum_{i=1}^{n}\sum_{j=1}^{k} m_j g = \left(\sum_{i=1}^{n}\sum_{j=1}^{k} m_j g\right)_H + \left(\sum_{i=1}^{n}\sum_{j=1}^{k} m_j(\alpha) g\right)_I \quad (5)$$

where $i = 1...n$ is the number of main chain component; $j = 1...k$ is the number of subcomponent.

Generally, tensile force of the chain $F_{t\Sigma}$ depends on weight force of chain F_c and conveyed material F_M:

$$F_{t\Sigma} = F_c + F_M \tag{6}$$

The structure of conveyor consists of horizontal and inclined parts. Therefore, the members in Eq. (6) may be separately written as

$$F_c = F_H + F_I\,,\ F_M = F_{HM} + F_{IM} \tag{7}$$

Using Eq. (7), Eq. (6) looks like this

$$F_{t\Sigma} = F + F_M = F_H + F_{HM} + F_I + F_{IM}\,. \tag{8}$$

2.2. Chain loading by its own weight

2.2.1. Horizontal chain part

Tensile force of chain when its strand hasn‘t a contact with the conveyor border

$$F_{cH} = 2\left[\left(G_c + G_h + G_b\right)N + G_a + G_p\right] f_r k_i \tag{9}$$

$$F_{cH} = 2gk_i f_r \left\{ \begin{array}{c} \left(\begin{array}{c} L_H q + n_H \times \\ \times \left(\begin{array}{c} \left(m_{hc} + m_{h\,p}\right) + \\ + \left(\begin{array}{c} m_{b1} + m_{b2} + \\ + m_{b3} + m_{b4} \end{array} \right) \end{array} \right) \end{array} \right) \times \\ \times N + n_H \left(m_a + m_p\right) \end{array} \right\} \tag{9.1}$$

Changing complex multiplier of Eq. (9.1) by Φ we get

$$\Phi = 2gk_i \left\{ \begin{array}{c} \left(\begin{array}{c} L_H q + n_H \times \\ \times \left(\begin{array}{c} \left(m_{hc} + m_{hp}\right) + \\ + \left(\begin{array}{c} m_{b1} + m_{b2} + \\ + m_{b3} + m_{b4} \end{array} \right) \end{array} \right) \end{array} \right) \times \\ \times N + n_H \left(m_a + m_p\right) \end{array} \right\}$$

and then (Eq. (9.1)) could be written in simple form

$$F_{cH} = \Phi f_r \tag{9.2}$$

Tensile force of chain when its strand contacts with the conveyor border

$$F_{cH} = 2\left[\left(G_c + G_h + G_b\right)N + G_a + G_p\right] \times$$
$$\times\left(f_r + \frac{\phi_H f_s}{2}\right)k_i;\ F_{cH} = \Phi\left(f_r + \frac{\phi_H f_s}{2}\right) \tag{10}$$

where $G_c = L_H qg$; $G_b = n_H\left(m_{b1} + m_{b2} + m_{b3} + m_{b4}\right)g$; $G_h = n_H\left(m_{hc} + m_{hp}\right)g$; $G_a = n_H m_a g$; $G_p = n_H m_p g$; $\phi_H = \frac{L_{cH}}{L_H}$; $n_H = NL_H P^{-1}$.

In Eq. (10), coefficient f_s changes according to operational conditions. Therefore, two different values of mentioned coefficient were used regarding the dry and wet cases f_{sd} and f_{sw}, respectively.

2.2.2. Inclined chain part

Tensile force of chain when its strand hasn‘t a contact with the conveyor border:

$$F_{cI} = 2\left[\left(G_c + G_l + G_V\right)N + G_k + G_j\right] \times$$
$$\times\left(f_r cos\alpha + sin\alpha\right)k_i;\ F_{cI} = \Phi'\left(f_r cos\alpha + sin\alpha\right) \tag{11}$$

Tensile force of chain when its strand contacts with the conveyor border

$$\left.\begin{array}{l} F_{cI} = 2\left[\left(G_{gr} + G_l + G_V\right)N + G_k + G_j\right] \times \\ \times\left(\left(f_r + \frac{\phi_I f_{tr}}{2}\right)cos\alpha + sin\alpha\right)k_i \\ F_{cI} = \Phi'\left(\left(f_r + \frac{\phi_I f_c}{2}\right)cos\alpha + sin\alpha\right) \end{array}\right\} \tag{12}$$

where $G_b = n_I\left(m_{b1} + m_{b2} + m_{b3} + m_{b4}\right)g$; $G_c = L_I qg$; $G_h = n_I\left(m_{hc} + m_{hp}\right)g$; $G_p = n_I m_p g$; $G_a = n_I m_a g$; $\phi_I = \frac{L_{cI}}{L_I}$; $n_I = NL_I P^{-1}$.

2.3. Chain loading by its own weight and weight of conweyed material

2.3.1. Horizontal chain part

Tensile force of chain when its strand hasn‘t a contact with the conveyor border

$$F_{cH} = \left\{ \begin{array}{l} 2\left[\left(G_c + G_h + G_b\right)N + G_a + G_p\right] \times \\ \times f_r + G_{MH} f_{sM} \end{array} \right\} k_i \tag{13}$$

In explicit form Eq. (15) looks like this

$$F_{cH} = 2gk_i \left\{ \begin{array}{c} f_r \left\{ \begin{array}{c} \left(\begin{array}{c} L_H q + n_H \times \\ \times \left(\begin{array}{c} \left(m_{hc} + m_{hp}\right) + \\ + \left(\begin{array}{c} m_{b1} + m_{b2} + \\ + m_{b3} + m_{b4} \end{array} \right) \end{array} \right) \end{array} \right) \times \\ \times N + n_H\left(m_a + m_p\right) \end{array} \right\} + \\ + \frac{1}{2} f_{sM} n_H m_M k_f \psi \end{array} \right\} \tag{13.1}$$

The complex multiplier is changed by Φ, then

$$F_{cH} = \Phi f_r + \frac{1}{2} f_{sM} n_H m_M g k_f \psi k_i \tag{13.2}$$

Tensile force of chain when its strand has a contact with the conveyor border

$$\left.\begin{aligned} F_{cH} &= \left\{\begin{aligned} &2\left[\left(G_c+G_h+G_b\right)N+G_a+G_p\right]\times \\ &\times\left(f_r+\frac{\phi_H f_s}{2}\right)+G_{MH} f_{sM} \end{aligned}\right\} k_i \\ F_{cH} &= \Phi\left(f_r+\frac{\phi_H f_s}{2}\right)+\frac{1}{2} f_{sM}\ n_H\ m_M\ g k_f \psi k_i \end{aligned}\right\} \quad (14)$$

where $G_{MH} = n_H PBH\rho g\psi k_f$.

2.3.2. Inclined chain part

Tensile force of chain when the chain strand hasn‘t a contact with the conveyor border

$$\left.\begin{aligned} F_{cI} &= \left\{\begin{aligned} &2\left[\left(G_c+G_h+G_b\right)N+G_a+G_p\right]\times \\ &\times\left(f_r cos\alpha+sin\alpha\right)+G_{MI}\times \\ &\times\left(f_{sM} cos\alpha+sin\alpha\right) \end{aligned}\right\} k_i \\ F_{cI} &= \Phi'\left(f_r cos\alpha+sin\alpha\right)+ \\ &+\frac{1}{2} k_i n_I g m_M k_f \psi\left(f_{sM} cos\alpha+sin\alpha\right) \end{aligned}\right\} \quad (15)$$

Tensile force of chain when its strand has a contact with the conveyor border

$$\left.\begin{aligned} F_{cI} &= \left\{\begin{aligned} &2\left[\left(G_c+G_h+G_b\right)N+G_a+G_p\right]\times \\ &\times\left(\left(f_r+\frac{\phi_I f_s}{2}\right)cos\alpha+sin\alpha\right)+ \\ &+G_{MI}\left(f_{sM} cos\alpha+sin\alpha\right) \end{aligned}\right\} k_i \\ F_{cI} &= \Phi'\left(\left(f_r+\frac{\phi_I f_s}{2}\right)cos\alpha+sin\alpha\right)+ \\ &+\frac{1}{2} k_i n_I g m_M k_f \psi\left(f_{sM} cos\alpha+sin\alpha\right) \end{aligned}\right\} \quad (16)$$

where $G_{MI} = n_I PBH\rho g\psi k_f$.

2.3.3. Coefficient of rolling resistance

Under good lubrication conditions with $\xi < 0.4$, rolling resistance coefficient is $f_r = 0.12$. When the inner surface of roller and external surface of axle worn down [1], then wood shavings fall between them, and at 100 % contamination by wood chips ($\xi = 1$), we have $f_r = 0.36$, which corresponds to the similar value of coefficient of sliding friction between two metallic surfaces in dry operational conditions – $f_{sd} = 0.35$. In the reference [3], the rolling friction coefficient is calculated as follows

$$f_r = \frac{2c+\xi f_{sM} d_{in}}{d_{ex}} \quad (17)$$

In this work the following codes of modeled loading scenario of conveyor were used: NL – non-loaded; NL/0 – non-loaded, distorted; NL/0.35 – non-loaded, distorted, dry friction; L10/0.35...L50/0.35 – loaded by 10...50%, distorted, dry friction; E – experimental value.

3. Experimental method

A distortion of chain strands was used in computation method procedure and compared with the experimental results organized using similar loading scenario and principal scheme shown in Fig. 3. Voltage and current waveforms were measured using USB data acquisition module Data Translation DT9816 with voltage transformer and current probe LEM PR200. Data acquisition module offers A/D resolution of 16 bits and simultaneous sampling of all six analogue input signals at up to 150 kHz per channel. These tools allow achieving less than 0.1% voltage and less than 1% current readout accuracy [6].

Active power consumed by the motor

$$P = 3UIcos\varphi \quad (18)$$

there $U = U_m/\sqrt{2}$, $I = I_m/\sqrt{2}$ are RMS values of voltage and current; U_m, I_m are amplitudes of voltage and electric current, respectively, and φ is the phase angle between the voltage and current.

The actuator force of transporter is evaluated by the following equation

$$F = \frac{P\eta}{v} \quad (19)$$

where η is the coefficient of efficiency of mechanical actuator; v is the linear chain velocity.

Obtained differences in the measured electric characteristics are shown in Fig. 4.

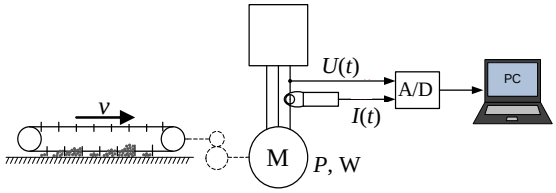

Fig. 3 Principal scheme on determination of electric power

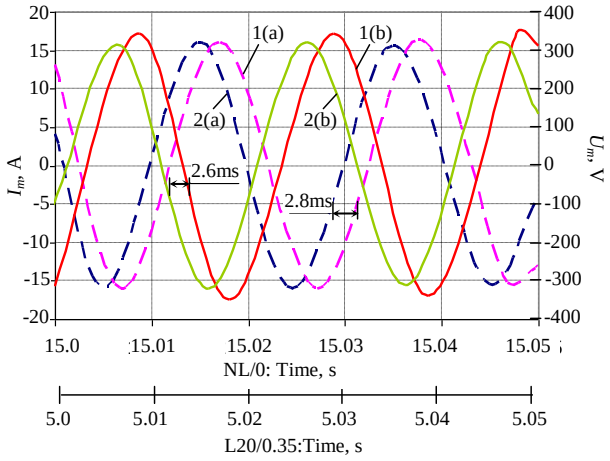

Fig. 4 Measurement data of electric characteristics: *1* - electric current, *2* - voltage; conveyor loading scenario: a - non-loaded (NL/0), b - loaded (L20/0.35)

Bracket values were obtained by the use Eq. (19) and were compared with analyticaly obtained results by Eq. (20) for the same loading scenario (Fig. 6).

Table 1

Measurement data of electric characteristics

Title of determined characteristic, measure units	Conveyor loading scenario	
	E-NL/0	E-L20/0.35
Velocity of chain, m/s	0.38	0.38
Current drawn by motor, A_{RMS}	10.3	12.1
Motor voltage, V_{RMS}	226.5	224.3
Apparent power consumption, kVA	6.9	8.1
Active power consumption, kW	4.5	5.58
Power factor $cos(\varphi)$	0.64.	0.69
Tensile force of actuator, kN	11.8 (11.2)	14.7 (13.9)

4. Exclusion of incidental load

In Fig. 5, the fragment of single chain strand is presented.

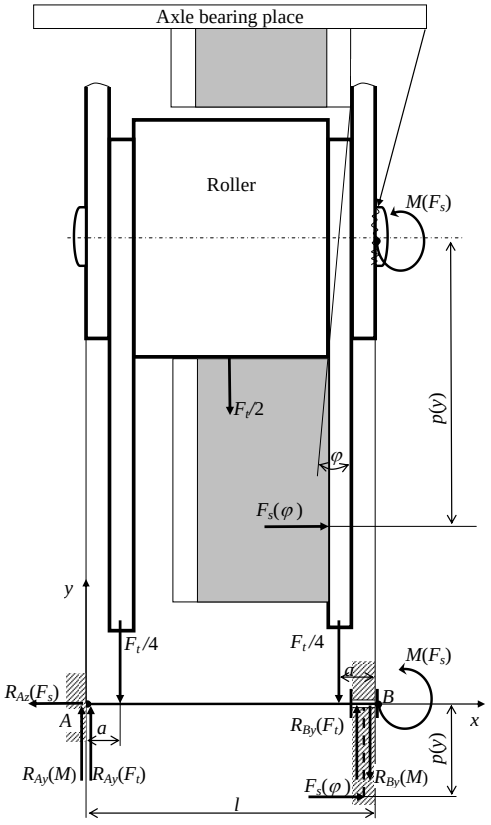

Fig. 5 Chain strand fragment and computational scheme showing balance of forces for chain members affected by resulting incidental loads $F_s(\varphi)$ and $M(F_s)$ in the case of angle $|\varphi| > 0$

The simplified computational scheme showing balance of forces for chain members affected by resulting incidental loads $F_s(\varphi)$ and $M(F_s)$, if $|\varphi| > 0$. Acording to the scheme presented in Fig. 6, tensile force, shear force and bending moment have following expressions

$$F_t\left(\varphi(y)\right) = \frac{F_{t\Sigma}}{N\cos\varphi(y)} \tag{20}$$

$$F_s\left(\varphi(y)\right) = \frac{F_{t\Sigma} tg\varphi(y)}{N} \tag{21}$$

$$M\left(p, \varphi(y)\right) = \frac{pF_{t\Sigma} tg\varphi(y)}{N} \tag{22}$$

In the case of straigth chain ($\varphi = 0$), $F_t(\varphi(y)) = F_{t\Sigma}$, $F_s\left(\varphi(y)\right) = 0$, $M(p, \varphi(y)) = 0$.

If chain segment wears on the tooth with the angle $\varphi \neq 0$, transversal loading of a chain segment occures and transversal force F_s starts to act. The product of this force F_s and chain segment pitch p generates bending moment $M(F_s)$ that bends a segment plate and axle, Eq. (22). The active loads are following: two longitudinal tensile forces $F_t/4$, Eq. (20); transversal force $F_s(\varphi(y))$, Eq. (21) and axle acting couple $M(F_s)$, Eq. (22). Support A has three constrains and support B – two ones. The results obtained by Eq. (20...22) are shown in Figs. 6-8.

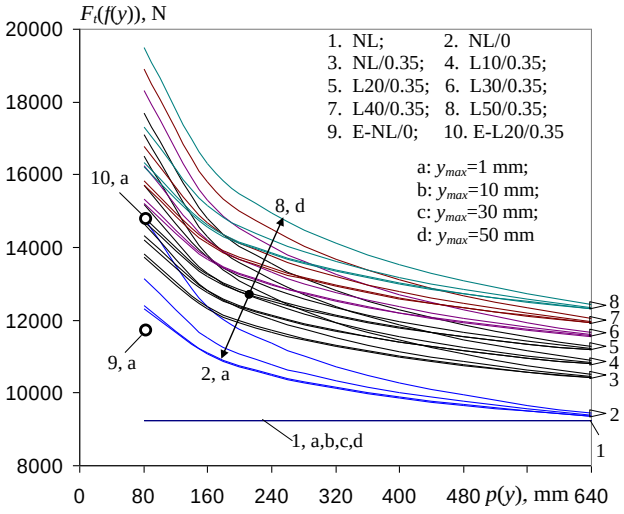

Fig. 6 Tensile force of chain $F_{t\Sigma}$ versus chain distance $p(y)$ influenced by scrapper deflection depth y_{max} and level of loading (Eq. 6)

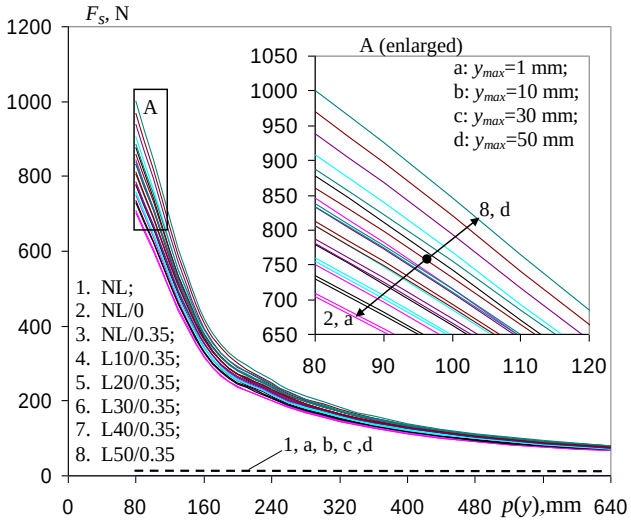

Fig. 7 Shear force of single chain strand F_s versus chain distance $p(y)$ influenced by scrapper deflection depth y_{max} and level of loading (Eq. 21)

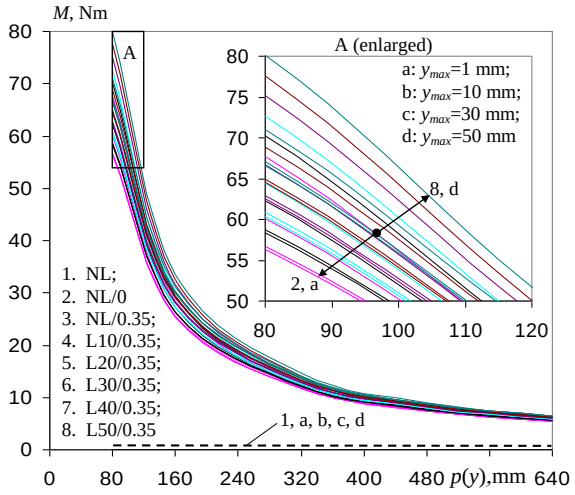

Fig. 8 Bending moment of single chain strand M versus chain distance $p(y)$ influenced by scrapper deflection depth y_{max} and level of loading (Eq. 22)

In calculations folowing input data were used: f_{sd} = 0.35, N = 2, k_i = 1.1, $p(y)$ = 80…640 mm, p = 80 mm, α = 50°, q = 15.33 kg/m^3, m_h = 0.687 kg, m_b = 0.115 kg, m_p = 6.0 kg, m_a = 4.586 kg, g = 9.81 m/s^2, B = 1000 mm, P = 640 mm, P = 80 mm, ρ = 250 kg/m^3, ϕ = 0.3, ψ = 0.75, k_f = 0…1, L_H = 12 m, L_I = 5 m, s = 8 mm, r_{ex} = 11 mm, r_{in} = 10 mm, ξ = 0.7, c = 0.6, f_{sM} = 0.8, d_{ex} = 70 mm, d_{in} = 30 mm, y_{max} = 1…50 mm, c_1 = 100…500 mm, η = 0.95, b = 10 mm, w = 10 mm, t = 10 mm.

5. Stresses on the axle

Bending moment $M(F_s)$ was replaced on the axle axis z around which the moment equation ΣM_z was written (Fig. 9). The objective was to calculate resultant shear force F_{sa} acting on the axle

$$\left.\begin{aligned}&\sum M_z = 0;\ F_{sa} y_c = M(F_s)\\ &F_{sa} = \frac{M(F_s)}{y_c} = \frac{3}{8}\frac{\left[\pi\left(r_{ex}^2 - r_i^2\right) - b\left(r_{ex} - r_i\right)\right] F_c\, ptg\varphi}{\left(r_{ex}^3 - r_i^3\right) - \frac{1}{8}b^2\left(r_{ex} - r_i\right)}\end{aligned}\right\} \quad (26)$$

Denominator of Eq. (26) represents the first moment of bearing area at the contact – $\frac{1}{12}\left(8\left(r_{ex}^3 - r_i^3\right) - b^2\left(r_{ex} - r_i\right)\right)$, and nominator $\frac{1}{2}\left(\pi\left(r_{ex}^2 - r_i^2\right) - b\left(r_{ex} - r_i\right)\right)$ - bearing area of the contact.

The representation of calculation results of resultant shear force F_{sa} acting on the axle is shown in Fig. 10.

For presented computational scheme (Fig. 5), the method of superposed loads was applied. Regarding presented boundary conditions and chosen method, the loads F_t and M were applied separetely. It allows us to simplify structure of equation and decrease number of members in it. Using longitudinal tensile force F_t the moment balance equations give results of reactive forces $R_{AY}(F_t)$ and $R_{BY}(F_t)$

$$\left\{\begin{aligned}&\sum M_A(F_t) = 0;\ \uparrow R_{BY}(F_t) = \frac{F_t}{2N}\\ &\sum M_B(F_t) = 0;\ \uparrow R_{AY}(F_t) = \frac{F_t}{2N}\end{aligned}\right. \quad (23)$$

Other load, bending couple $M(F_s)$ and moment balance equations give other two reactive forces $R_{AY}(M(F_s))$ and $R_{BY}(M(F_s))$.

$$\left\{\begin{aligned}&\sum M_A\left(M(F_s)\right) = 0;\ \downarrow R_{BY}\left(M(F_s)\right) = \frac{M(F_s)}{l}\\ &\sum M_B\left(M(F_s)\right) = 0;\ \uparrow R_{AY}\left(M(F_s)\right) = \frac{M(F_s)}{l}\end{aligned}\right. \quad (24)$$

Here, the arrows ↑ and ↓ mean reaction directions „upsters“ and „downsters“, respectivelly.

To be sure that reaction forces were calculated correctly the following balance equation of forces is used

$$\left.\begin{aligned}&\sum F_Y\left(F_t, M(F_s)\right) = 0\\ &-R_{AY}\left(M(F_s)\right) + R_{AY}(F_t) - \frac{F_t}{2N} - \frac{F_t}{2N} + R_{BY}(F_t) + R_{AY}\left(M(F_s)\right) = 0\\ &\frac{M(F_s)}{l} + \frac{F_t}{N} = \frac{M(F_s)}{l} + \frac{F_t}{N}\end{aligned}\right\} \quad (25)$$

Accordingly, excluded incidental loads F_s and M can be used in calculations of stresses.

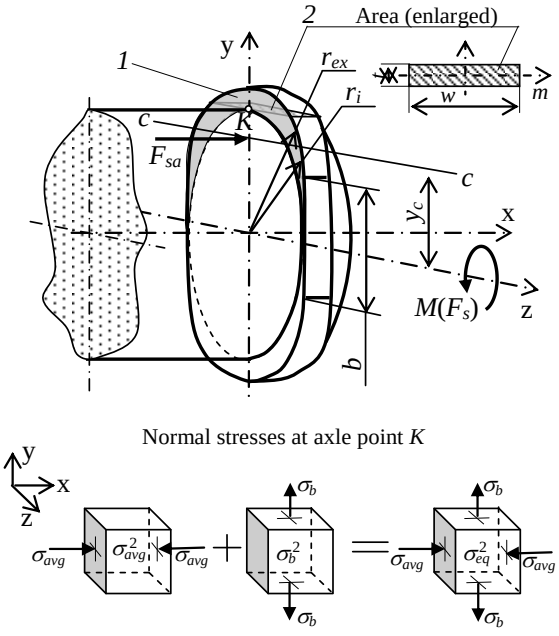

Fig. 9 Axle areas showing an existance of normal stresses in bearing (σ_{avg}) and in bending (σ_b) caused by resultant shear force F_{sa} and bending couple $M(F_s)$, respectively: *1* – area of bearing; *2* – cross-sectional area of bending

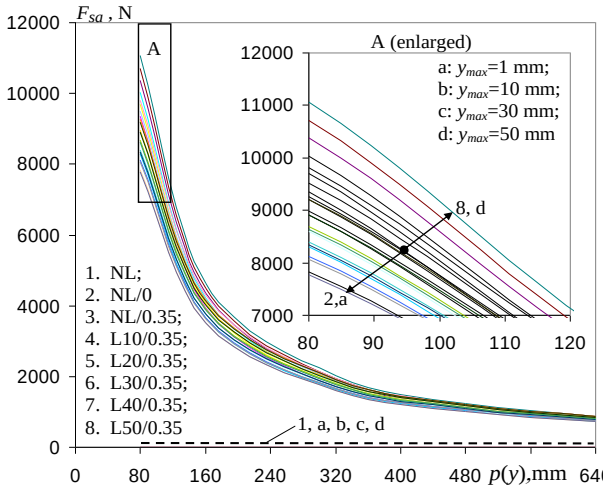

Fig. 10 Shear force on axle F_{sa} versus chain distance $p(y)$ influenced by scrapper deflection depth y_{max} and level of loading Eq. (26)

Force F_{sa} increases mostly, if scrapper comes close to teeth of drive sprocket.

According to presented working condition chain axle is act on bearing and on bending. So, the stresses were denoted as follows σ_{avg} and σ_b. Stress state at point K is shown in Fig. 9. Equivalent stress σ_{eq} at point K represents a geometric sum that joins both normal stresses: averraging bearing stress σ_{avg} and bending stress σ_b

$$\sigma_{eq} = \sqrt{\sigma_{avg}^2 + \sigma_b^2} = \sqrt{\sigma_x^2 + \sigma_y^2} \tag{27}$$

Such loading conditions mentioned above were compared with Mises yield criterion for stresses [7]. As it could be seen, according to presented load scenario, stress state also may represent following principal stresses $\sigma_{avg} = \sigma_x = \sigma_1 \neq 0$ and $\sigma_b = \sigma_y = \sigma_2 \neq 0$, where $\sigma_1 < 0$ and $\sigma_2 > 0$. Other stress members were used with the restrictions $\sigma_3 = 0$, $\tau_{12} = \tau_{13} = \tau_{23} = 0$ and ones weren't taken into account.

In the case of principal stress, applying simplified von Mises yield criterion at axle point K, we get

$$\sigma_\upsilon = \sqrt{\frac{1}{2}\left[\left(-\sigma_1 - \sigma_2\right)^2 + \left(-\sigma_1\right)^2 + {\sigma_2}^2\right]} \tag{28}$$

In explicit form, the average of normal stress in bearing could be written as

$$\sigma_{avg} = \frac{F_{sa}}{A} = \frac{\frac{3}{8}\left[\pi\left(r_{ex}^2 - r_i^2\right) - b\left(r_{ex} - r_i\right)\right]F_c p}{\left(r_{ex}^3 - r_i^3\right) - \frac{1}{8}b^2\left(r_{ex} - r_i\right)} tg\varphi = \frac{\frac{1}{2}\left[\pi\left(r_{ex}^2 - r_i^2\right) - b\left(r_{ex} - r_i\right)\right]}{\left(r_{ex}^3 - r_i^3\right) - \frac{1}{8}b^2\left(r_{ex} - r_i\right)} = \frac{3F_c p tg\varphi}{4\left[\left(r_{ex}^3 - r_i^3\right) - \frac{1}{8}b^2\left(r_{ex} - r_i\right)\right]} \tag{29}$$

Axle moment influences on normal stress σ_b caused by bending. Such stress is expressed as follows

$$\sigma_b = \frac{6M\left(F_s\right)}{wt^2} \tag{30}$$

Eqs. (27)-(30) presents results shown in Fig. 11.

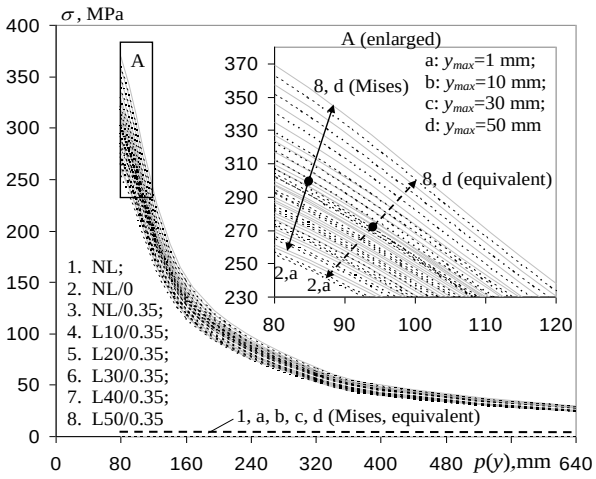

Fig. 11 Normal stresses on the axle versus chain distance $p(y)$ influenced by scrapper deflection depth y_{max} and level of loading; solid line – von-Mises stress σ_υ and dashed line – equivalent stress σ_{eq}, Eq. (27) and Eq. (28)

6. Conclusions

The primary factors that led chain to start to come into contact with the conveyor frame could be asymmetrical distribution of conveyed fuel in the transport plane or the tilt of runners. Chain distortion happens yielding bad fuel and hitting the scraper. Drive shaft axis may have an inclination in relation to the horizontal plane and frontally. Chain durability depends mostly on angle φ. It increases further if scraper was dent previously and distance between the chains decreased. One of both chains during the same period of time will be much weaker than another. During operation chain distortion is the emergence of shear force $F_s(\varphi)$ that causes bending moment $M(F_s)$ and bearing in the chain axle head and plate exuviations from it, too. External force F_{sa} acting on the narrower chain segment with scraper step distance p = 80 mm is about 10 times greater than remote segment with the scraper step distance p = 640 mm. Stress σ_1 on the axle head of the chain is basically crucial and it comes close to ultimate stress σ_u (Figs. 11 and 12).

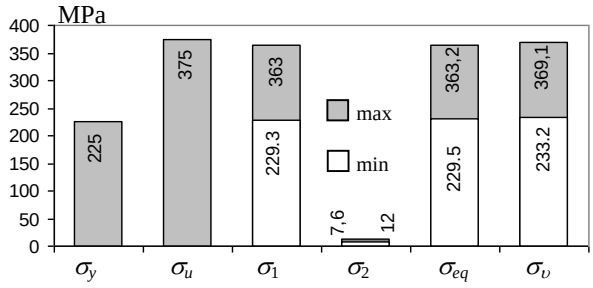

Fig. 12 Comparative analysis of stresses related with mechanical properties of axle material and analytically obtained values of stresses σ_1 and σ_2

Also, products of contamination by small particles of wood chips and corrosion had influenced on the increase of coefficient f_r and stresses σ_{eq} and σ_{υ}.

References

1. **Gustavsson, F.; Forsberg, P.; Jacobson, S.** 2012. Friction and wear behaviour of low-friction coatings in conventional and alternative fuels, Tribology International. Volume 48, April, 22-28. http://dx.doi.org/10.1016/j.triboint.2011.06.001.
2. **Rašimaitė, T.** 2012. Lithuania among the cleanest countries in the world, Journal „Savaitė“ No.6, 6 p. (in Lithuanian).
3. http://epi.yale.edu/epi2012/methodology (2012 04).
4. http://www.jungbluth–ketten.de/downloads /EN/jungbluth_main_catalogue.pdf (2012 04)
5. Handbook of Reliability Prediction Procedures for Mechanical Equipment. Carderockdiv, NSWC-11. – 2011.
6. **Augutis Stasys Vygantas; Nakutis Žilvinas; Ramanauskas Ramūnas** 2009. Advances of Barkhausen emission measurement, IEEE Transactions on Instrumentation and Measurement, Piscataway: IEEE Instrumentation and Measurement Society, 58(2): 337-341.
7. **Bereiša, M.; Žiliukas, A.; Leišis, V.; Jutas, A.; Didžiokas, R.** 2005. Comparison of pipe internal pressure calculation methods based on design pressure and yield strength, Mechanika 4(54): 5-11.

A. Žiliukas, S. Diliūnas, A. Jutas, S.V. Augutis, R. Ramanauskas

EKSPLOATACIJOS METU PERKRAUTŲ BIOKURO KONVEJERIO GRANDINĖS ELEMENTŲ STIPRUMO UŽDAVINYS

R e z i u m ė

Nedideli nukrypimai nuo grandinių eksploatavimo sąlygų daro poveikį įvairiems jų deformavimo atvejams, kurie neminimi grandinių eksploatacijos nurodymuose. Net ir labai mažai persikreipusi grandinė yra veikiama skersinės jėgos ir lenkimo momento. Šios papildomos apkrovos padidina grandinės ašelės įtempių skaitinę vertę, kuri kritinio apkrovimo metu pasiekia ašelės medžiagos stiprumo ribą. Šiame straipsnyje pateikiama originali atlikto tyrimo metodologija, įvertinanti grandinės eksploatacinės kinetikos įtaką jos geometriniams ir mechaniniams rodikliams. Susiję matavimo ir skaičiavimo rezultatai buvo panaudoti pateiktai metodologijai patikrinti.

A. Žiliukas, S. Diliūnas, A. Jutas, V. Augutis, R. Ramanauskas

ON THE STRENGTH PROBLEM IN CHAIN ELEMENTS OVERLOADED DURING MAINTENANCE OF BIO-FUEL CONVEYOR

S u m m a r y

Small deviations in maintenance conditions of chains influence on various cases of deformations that usually are not mentioned in the chain maintenance guide. In the case of small distortion of chain axis the chain is loaded by transversal load and chain elements incur a bending moment. These additional loads increase stress value on area of chain axle and it comes close to the value of ultimate stress. In this article the original evaluation methodology of geometrical and mechanical characteristics is presented according to chain loading kinetics. Also this article covers related measurement and calculation results that were used as tools for verification of presented methodology.

Keywords: Strength, chain conveyor, bio-fuel.

Received January 04, 2012
Accepted December 11, 2012